SAND2012-5975C

Damage Assessment of Composite Honeycomb Material Using Advanced Inspection Technologies

David G. Moore, and Ciji L. Nelson
Sandia National Laboratories
Nondestructive Evaluation and Experimental Mechanics Department
Post Office Box 5800 MS-0557
Albuquerque, New Mexico 87185

ABSTRACT

An in-situ advanced infrared inspection technique has been developed to detect in-service damage in solid laminate to honeycomb composite materials. Cell wall crushing and delamination between solid laminate/honeycomb interfaces is investigated. Comparisons between advanced ultrasonic inspection methods, computed tomography and active infrared technologies are discussed. A review of reference standard development, inspection criteria and deployment challenges encountered while scanning the honeycomb materials to detect discontinuities with active infrared technologies will also be examined. Finally, the results of reference standard development aided by both computed tomography and high speed ultrasonic inspections as a verification method will be presented.

1. INTRODUCTION

During the last several years, solid laminate to honeycomb structures are being studied at Sandia National Laboratories due to their unique structures and potential for aerospace applications [1 – 3]. The geometry of a honeycomb composite allows designers to minimize the amount of material used and still maintain weight/strength to cost ratios. The geometry of honeycomb structures vary widely within aerospace structures however, all contain common features. Honeycomb structures have a uniform two-dimensional array of hollow cells formed between two thin vertical walls that are bonded with adhesive. The cells are usually hexagonal in shape and are sandwiched between two solid laminates. Newer design shaped honeycomb structures provide a material with minimal density and relative high out-of-plane compression and shear properties. Manufactured honeycomb structural materials are commonly made by layering a honeycomb material between two thin layers of solid laminates that provide strength in tension. This forms a plate-like assembly. Honeycomb materials are widely used where flat or slightly curved surfaces are needed. The high strength-to-weight ratio makes this material useful during the design phase of projects. Sandia National Laboratories is studying advanced infrared inspection techniques for new composite applications. The composite panel specimen used in this evaluation is 20.32 by 20.32 cm and is composed of a Nomex™ honeycomb structure sandwiched between two laminate weave skins. The skin is composed of woven carbon fiber sheet material and is 3 plies thick [4, 5]. To help assess reference standard development and inspection criteria limits, the specimen was design with three embedded engineered flaws. These flaws simulate common flaws found during layup production.

The flaw types are disbonds, which are loss in adhesion between the laminate and the honeycomb core, and interplay delaminations, which are a loss in adhesion between adjacent plies of carbon laminate honeycomb. An assessment of each inspection technique was conducted to determine if an inspection criterion can be established. To assure damage is assessed correctly with infrared technology, several advanced inspection techniques were used to characterize material homogeneity.

1.1 Ultrasonic Inspection of Honeycomb Structure

Ultrasonic transducers transmit low or high frequency sonic waves into a composite sample and measure the response returned from the material. A change in the sonic vibrations indicates a structural change in the specimen due to a strong anisotropy between the axis and the plane of the stack [6]. Low-frequency ultrasonic transducers (resonant) transmit ultrasonic waves that penetrate through the laminate weave face and enter the honeycomb cell wall at the node bond adhesive interface. The low frequency response of the transducer can detect disbonds within the honeycomb and the laminate. Resonance inspection requires a highly resonant, narrowband transducer that can be excited at its natural resonant frequency and creates a tuned continuous standing wave (110 kHz). This inspection method requires an ultrasonic coupling agent (deionized water) between the transducer and the composite material. Water, a low-viscosity coupling material, was forced through a small tube near the probe tip and transferred to the inspection surface. Since the thickness of the part influences the acoustic impedance, relative measurements were made between an unflawed area and the remaining regions of the part. When the transducer approaches the edge of the part, a sharp change in resonant frequency occurs at the boundary condition. This condition limits inspection near the edge of the sample. In general, is it not advisable to inspect any closer than 3 mm from an edge. The resonant technique will not be able to discern a defect (change in structural stiffness) from the edge of the part.

High-frequency ultrasonic transducers have better resolution than low-frequency transducers, and primarily detect delaminations between the face adhesive interfaces. These types of defects are not very deep within the structure. To maximize acoustic energy into a material, the air between the ultrasonic transducer and the composite must be removed. Couplant removes the air and transfers the sonic energy from the probe into the material under test. This technique creates a robust and repeatable inspection to interrogate the composite to honeycomb bondline interface. In immersion testing, the part and the transducer are placed in a tank filled with water. This arrangement allows better movement of the transducer while maintaining consistent coupling. Its disadvantage is that the part must be submerged for long periods of time and the sample will likely absorb water. To avoid immersing the part in water, a manual contact method was developed. A couplant such as water, oil or a gel is applied between the transducer and the sample. The technique is manual and labor intensive. The honeycomb has an affinity for moisture. A way to improve near surface resolution with a single element transducer is through the use of a delay line. Delay line transducers have a polymer standoff that is located in front of the transducer. This provides a time delay between the acoustic generation and reception of reflected energy. The standoff essentially becomes the front surface of the composite and it also encompasses the constructive/destructive wave fronts and gives better near surface resolution. A small hole next to the transducer provides water to only the surface of the part through a water delivery system and allows the inspection to become automated.

1.2 Computed Tomography Inspection on Honeycomb Structure

The computed tomography is an x-ray imaging technique that generates an image of a thin slice of an object's volume. This technique differs from the other two described techniques in that the x-ray source lies in the same plane as the surface being imaged. Since the plane of the CT image is parallel with the beam and the detector scan path, all CT systems require computer algorithms to reconstruct, calculate, locate, and display pixel by pixel attenuation values throughout the honeycomb sample. The reconstruction is obtained by using the cross sectional slices of the test piece. The CT image represents a point-by-point linear attenuation coefficient in each slice which can then be correlated to the density. The computer software program Volume Graphics™ was used to characterize the honeycomb integrity by displaying planes of reconstructed data through the volume. Computed Tomography is an advanced radiographic method which is being used during product and process design optimization [7]. This technique can verify honeycomb structural characteristics after any manufacturing steps. Processes steps such as core-to-core splices, and core-to-structure splices are routinely detected. The CT technique is especially well suited for detecting sub-surface flaws within the honeycomb. The general types of defects detected by radiologic examination include blown core, core corrosion, density variation, entrapped fluid, and porosity or voids. Factors that influence image formation and X-ray attenuation and interpreting the images are the keys to successful deployment.

1.3 Infrared Inspection on Honeycomb Structure

Infrared (IR) inspection uses a video camera to image the surface of the honeycomb after the application of a short pulse of heat. The heat is applied by high-power xenon flash lamps. The camera and flash lamps are connected and controlled through an integrated computer system. This system is highly portable, as well as suitable for mechanical fixturing. The computer is used to process the digital video data stream from the IR camera, as well as to display the resulting images. The infrared imaging requires only a few seconds per square foot of surface. Camera focusing and lens selection can increase or decrease the field of view. The system is also capable of detecting and measuring material loss. This technique has been applied to detect: 1) disbonded metal-to-metal aircraft doublers 2) disbonds and delaminations in graphite and boron fiber composite structures and 3) characterize impact damage on a ply-by-ply basis in a carbon fiber composite [8]. Active Thermography (AT) is defined as a technique where a stimulus is applied to a sample to cause it to heat or cool locally. This local heating will allow the thermal characteristics of the sample to be observed by infrared imaging. The difference between active from passive thermography is the intentional application of heating, cooling or other excitation method that results in a temperature rise or fall in a sample, as compared to an otherwise in situ (passive) sample. In active thermography, the thermal response of a sample to a heating (or cooling) event is analyzed to determine the subsurface structure or material properties of the sample. The time at which temperature changes take place is often more important than the amplitude of the temperature change.

2. EXPERIMENTATION

2.1 Sample Characteristics

Figure 1 shows location of three engineered defects with the composite. The sample was constructed with a 12.7 mm thick nomex honeycomb sandwiched between three plies of plain weave carbon fiber sheet cloth [0,45,- 90]. Figure 2 displays a side view of the sample. Core

material was removed and excessive epoxy replaced it. The flaws are located on one side of the composite panel. There are three flaws with the following dimensions: 1) 25.4 mm diameter potted honeycomb core; 2) 2.54 by 2.54 cm square and 3) 12.7 mm diameter. Each shim was placed between the adhesive bond layers and coated with mold release to simulate a disbond.

2.2 Ultrasonic Inspection

Inspections were performed in order to observe capabilities and limitations of inspection technologies as well as determine if the engineered flaws will make suitable reference standards. The sample was ultrasonically inspected using a 6.35 mm diameter probe operating at 5 MHz. The scanner resolution was set to 0.5 mm. The gate was adjusted to follow the front surface and stop close to the backwall of the laminate weave skins. Figure 3 displays the inspection set-up using and advanced automated ultrasonic scanning system MAUS V™. Penetration of ultrasonic acoustic energy through the weave material to the honeycomb surface is shown in both amplitude and time of flight. If higher probe frequencies are used the resolution at the bond line may be detected. However, as frequency increases sound attenuation is greater and depth information can be lost. Figure 4 is an amplitude c-scan image of the laminate shin to the honeycomb. This image detects the change in acoustic density between the solid weave and honeycomb. All three engineered defects can be detected.

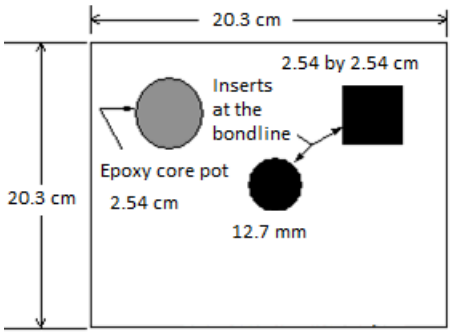

Figure 1. Honeycomb sample with defined engineered flaws.

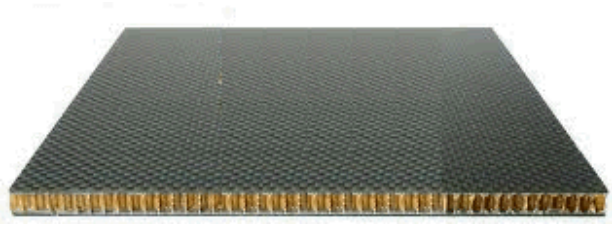

Figure 2. The panel is composed of Nomex™ honeycomb sandwiched between two laminates.

Figure 5 shows the ultrasonic inspection results of the honeycomb sample using c-scan depth gate display with a clear indication of the large square insert located at the top right. The 12.7 mm insert is barely detectable. A resonant inspection was also conducted on the sample. A 110 kHz resonance probe could not reliably detect the disbonds, however, the epoxy filled core was detected. The resonance probe was moderately successful and the image produced with it is shown in Figure 6. The high frequency scan could detect near-side delamination and disbonds. However, the signal strength diminished with depth of the honeycomb thickness. When the sample was flipped over, only the potted honeycomb core was detected. Around the perimeter of the flaws, the signal was attenuated. Using the resonant inspection method, a plot of phase changes assisted with data interpretation (Figure 7). The phase change can indicate either a change in depth or thickness of the ply. When establishing criteria for resonant inspection these may or may not be considered defects therefore this type of defect may not be usable as a reference standard.

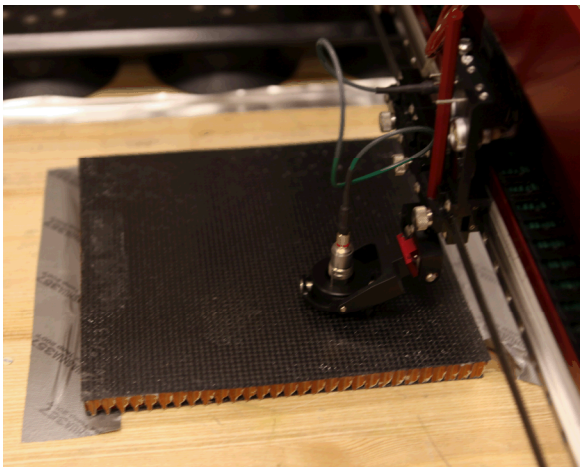

Figure 3. A 5 MHz probe coupled the advanced automated ultrasonic scanning system MAUS V™.

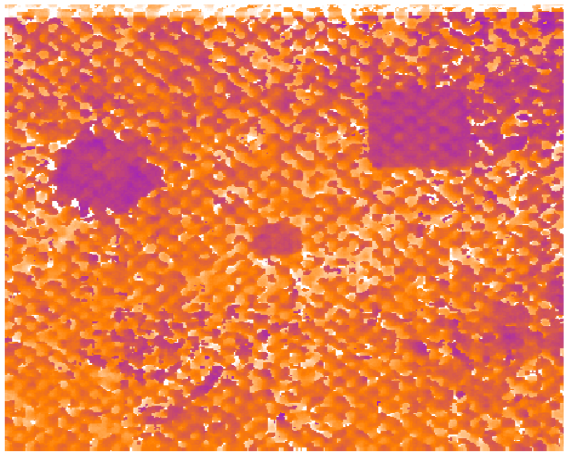

Figure 4. Screen display of c-scan image. The signal amplitude in the gate is recorded and displayed.

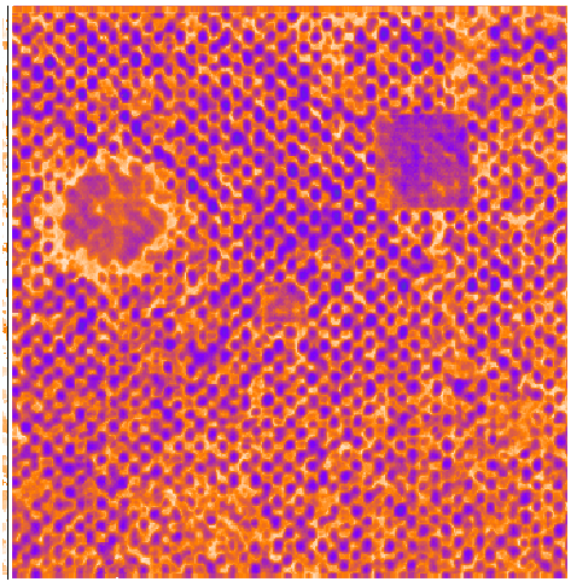

Figure 5. Screen display of c-scan image. The depth within the gate is recorded and displayed.

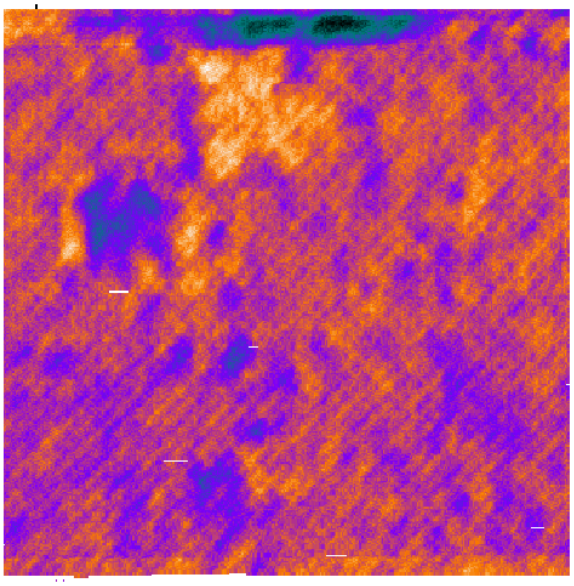

Figure 6. Screen display of c-scan image. The amplitude response for resonant probe is recorded and displayed.

The inspection data shows that resonant inspection has some limitations in defining the shape/borders of these type of flaws however; it was possible to detect the presence of a flaw. Large signal variations were found at the surface of the bondline between the face and honeycomb using resonant techniques. These variations may be the result of irregularities in the composite cloth material or the fabrication process.

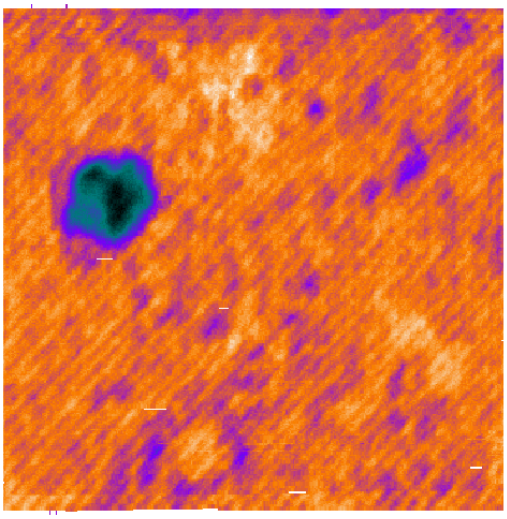

Figure 7. Screen display of c-scan image. The phase response for resonant probe is recorded and displayed.

2.3 Computed Tomography Inspection

The computed tomography (CT) technique developed for this sample collects penetrating radiation measurements from the honeycomb's x-ray opacity using an amorphous silicon digital detector array (flat panel). The source and detector remained constant while the part was scanned and indexed. These slices were than collected and mapped together to create a two dimensional CT-density map. The fraction of the x-ray beam that is attenuated is directly related to the density and thickness of the material through which the beam has traveled. Figure 8 pictorially displays the technique.

Volume Graphics software generates three-dimensional images from the set of two-dimensional measurements at different scanning angles. The reconstruction algorithm uses a transform technique which uses a continuous set of voxels arranged in a three-dimensional grid. Each voxel represents a specific area of the composite honeycomb structure. The "gray" values assigned correlates to the material properties of the area.

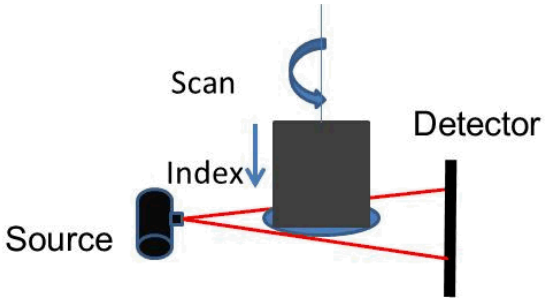

Figure 8. Computed tomography setup for a honeycomb sample.

Figure 9 shows the texture of the surface of the weave (facing sheet). Figure 10 displays the laminate to bondline interface. The honeycomb cell structure is well defined. As the computed tomography slice continued through the honeycomb, crushed and condensed core damage was

detected at approximately half way through the sample. Figures 11 and 12 display the front and side view slide plane at the core damage site. A Perkin Elmer (2048 by 2048 pixels) amorphous silicon flat panel with a 0.20 by 0.20 mm pixel pitch was used to collect the x-ray opacity. The panel to detector distance was placed at 1.5 meter to create an approximate 1-to-1 scale. The x-ray source operated at 160 Kilovolts with a current of 4.4 µA.

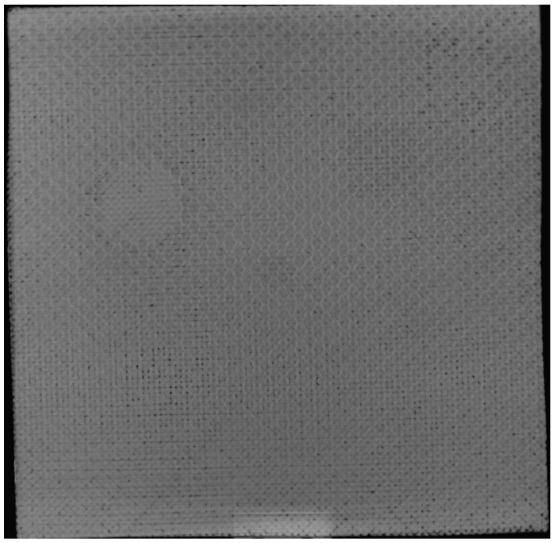

Figure 9. Computed tomography slice of the front surface showing the 3 ply layup.

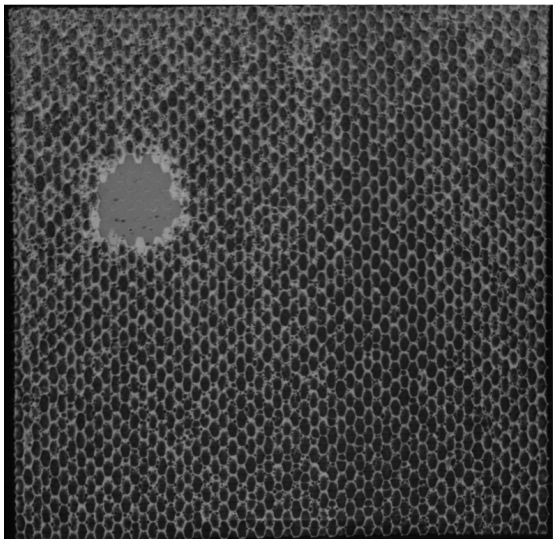

Figure 10. Computed tomography slice of the skin-to-honeycomb interface.

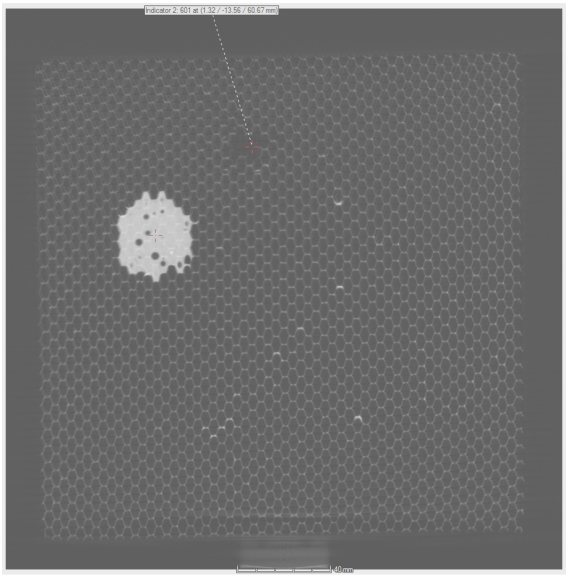

Figure 11. Computed tomography slice of the front surface showing cell wall crushing.

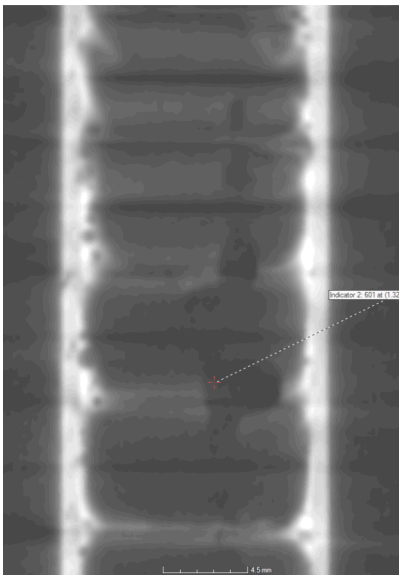

Figure 12. Computed tomography slice of the side view showing cell wall crushing.

2.4 Infrared Inspection

The use active infrared technology was deployed to assess its ability to detect disbond and delaminations between the laminate and composite honeycomb interface and determine if these types of engineering defects can be used as reference standards. A commercially available infrared system from Thermal Wave Imaging was used during this investigation [9]. To better understand where artifacts and variations in the processed infrared images come from, a subsystem analysis was conducted. The AC coupling effects, scene content, gain levels of the camera, and line to line interpolations were studied in order to optimize the set-up. To obtain the best image quality, the background temperatures and reflections were kept to a minimum. A short, quick thermal pulse (5 to 10 milliseconds) was applied to the sample. To avoid recording infrared camera saturation, data collection was delayed by 0.15 seconds. The camera frame rate was 59.9 Hz with a capture time of 21.2 seconds. The diffusion rates into the honeycomb are uneven due to air pockets and adhesive build up near the laminate to honeycomb interfaces. To assist with data analysis, a Thermographic Signal Reconstruction (TSR) algorithm was applied to the saved images. The algorithm fits the raw log-log data with a smoothing function and uses the replica for additional processing. Once the equations of fit are placed in the log domain, a transform can be created and stored. Presently, the two most useful functions are the first and second derivative. Figures 13 – 15 with the associated plots, illustrate pixel intensity per log time, along with the first and second derivatives of each chosen pixel within the collection window. Any data point (pixel intensity) within the collection time can be displayed. As time increases, the thermal response throughout laminate and honeycomb material can be analyzed.

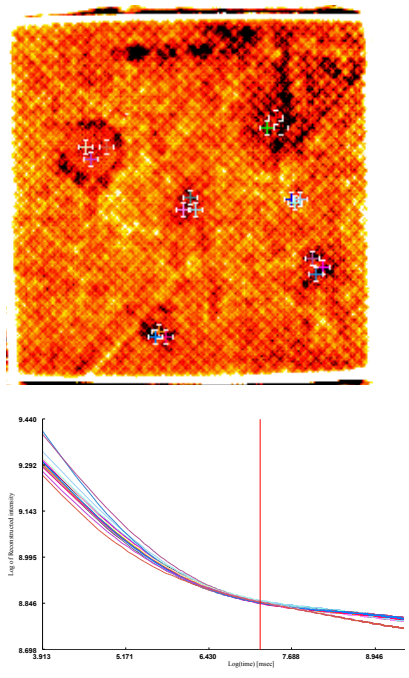

Figure 13a. Log of reconstructed intensity per unit log time (1.35 seconds).

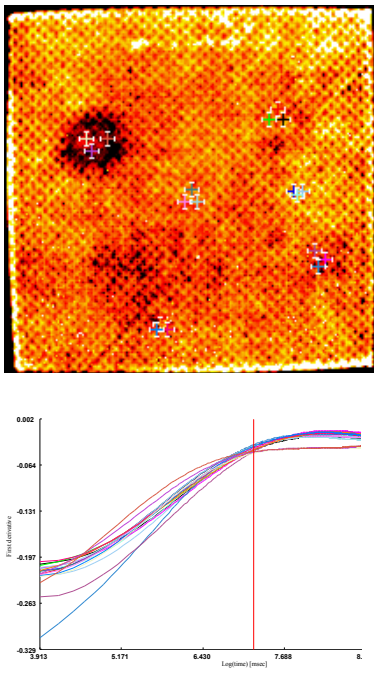

Figure 13b. First derivate of reconstructed intensity per unit log time (1.35 seconds).

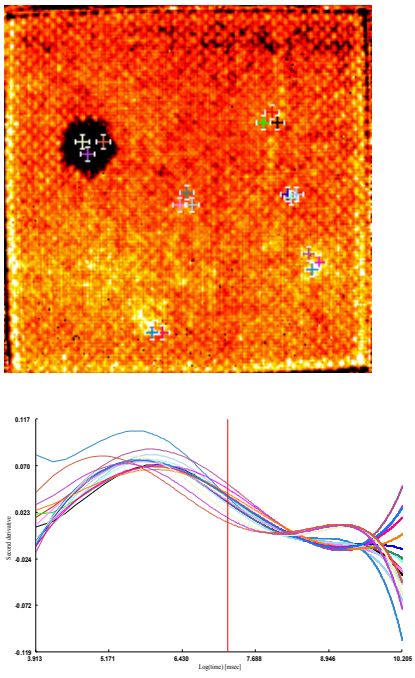

Figure 13c. Second derivate of reconstructed intensity per unit log time (1.35 seconds).

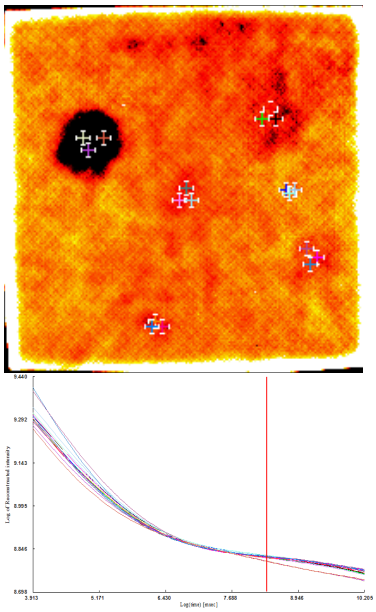

Figure 14a. Log of reconstructed intensity per unit log time (4.22 seconds).

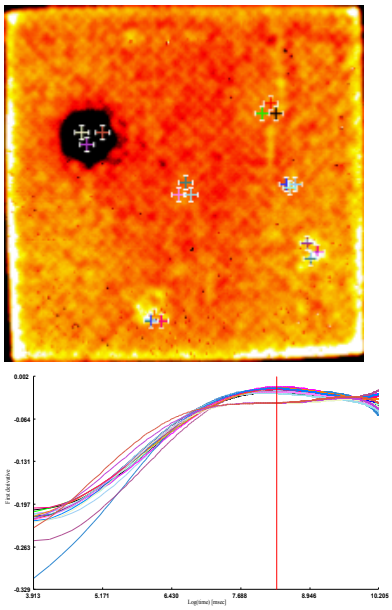

Figure 14b. First derivate of reconstructed intensity per unit log time (4.22 seconds).

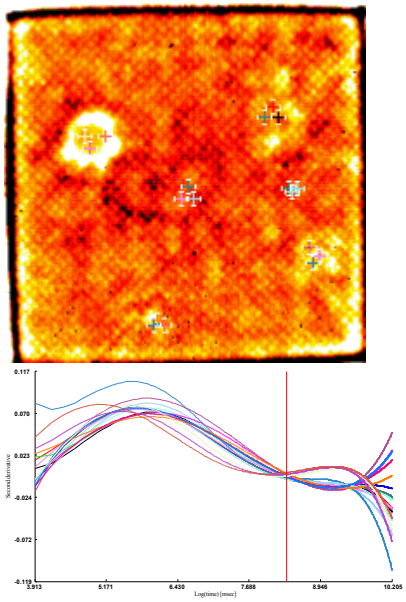

Figure 14c. Second derivate of reconstructed intensity per unit log time (4.22 seconds).

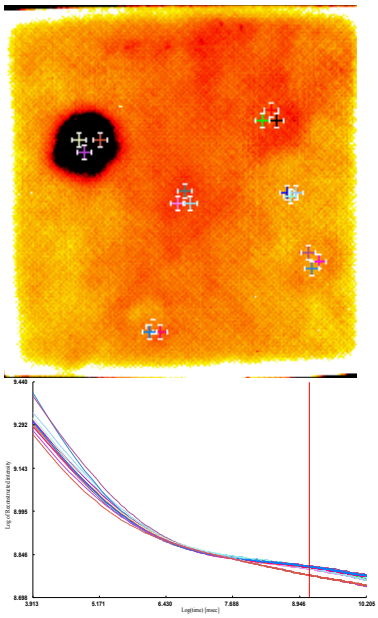

Figure 15a. Log of reconstructed intensity per unit log time (9.28 seconds).

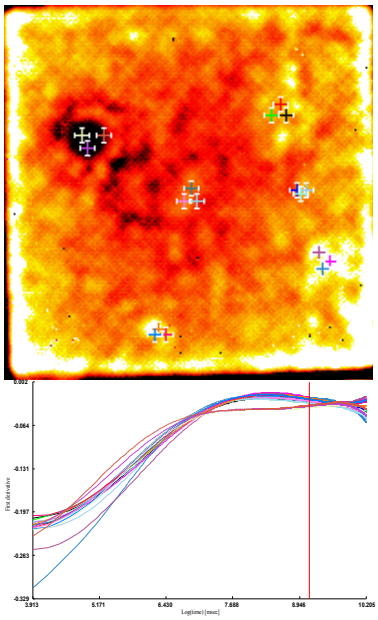

Figure 15b. First derivate of reconstructed intensity per unit log time (9.28 seconds).

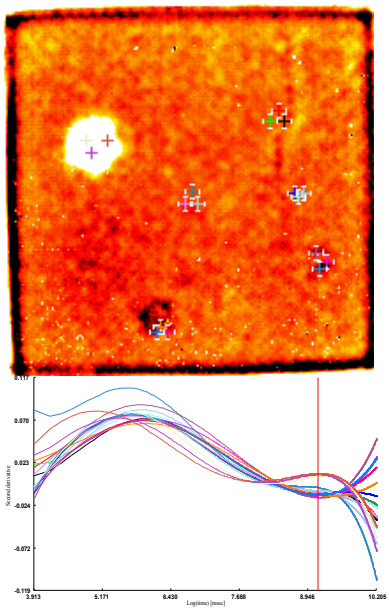

Figure 15c. Second derivate of reconstructed intensity per unit log time (9.28 seconds).

3. RESULTS

Increasing the ultrasonic frequency will increase the resolution of the ply to ply inspection. This variable change is thought to be able to delineate the honeycomb separation from the 3-ply weave and characterize fiber integrity. However, higher frequency scans will be inadequate for detecting defects near the honeycomb cell walls. Ultrasonic resonant inspection can detect near surface delaminations in this multilayer composite laminate bonded to honeycomb but cannot quantify the severity. This technology is able to detect the presence of a flaw; however, it has difficulty establishing the shape and extent of the flaw due to acoustic impedance mismatch caused by the presence of air gaps in the honeycomb structure.

The composite panel showed significant variation in all three inspection methods. However, computed tomography was a valuable assessment tool for evaluating through the thickness of the honeycomb material as well as the ply to ply variations. Presently, there is no known reference standard available for digital x-ray to compare the inspection results.

If the composite surface is shiny then light will be reflected from it. This may not allow enough heat to be deposited into the honeycomb surface and results are a low infrared signal. In this sample, the surface was shiny, however; the IR emissivity and optical absorption were enough to produce interpretable data. In these experiments, the derivatives remove reflection artifacts from the composite surface that appear in the raw image. The slope processing features extract most of the required data however; when the sample is inspected over and over it will retained some heat. This local heating effect can be removed in the TSR process or by subtraction pre-flash images. If the log plot of a defect free point is extremely distorted then reflected radiation is the predominate signal.

4. CONCLUSIONS

It is difficult to produce a reference standard that represents node bond degradation along the core ribbon direction and cell wall crushing. The only technique to characterize crush condensed core damage was computed tomography. Lack of adhesion at the skin-to-core bond can be represented by adding mold release agents to a shim prior to the debulking operation. However, the detection of the shim interface might be easier to detect than an actual processing discontinuity.

Core potting is an excellent way to produce a reference standard that will represent splices or honeycomb repair. All inspection techniques were able to detect this processing condition. An important requirement for reliable ultrasonic inspections is to maintain a constant ultrasonic beam entry angle throughout the whole inspection. Flat samples are easier to inspect however, complex 3D shapes require more advanced scan plans in order to be properly inspect and record reliable time of flight data.

Inserts at the bondline were identifiable with infrared inspection however, could not be used as a reference standard. Signal processing algorithms were used to enhance detectability of the inserts. All far surface flaws (the sample flipped over) could not be detected. Far surface flaws

are approximately 12.7 mm deep through the honeycomb and are beyond the realm of pulsed thermography. Ongoing research will investigate additional engineered flaws and determine the limitations of infrared techniques.

5. REFERENCES

1. Roach, Dennis, Rackow, Kirk, Sandia National Laboratories, FAA Airworthiness Assurance Center, "Improving In-Service Inspection of Composite Structures –It's a Game of CATT and MAUS", 7th Joint DoD/FAA/NASA Conference on Aging Aircraft, September 8-11, 2003, New Orleans, USA.
2. Valley, Mike T., Roach, Dennis P., Dorrell, Larry R., "Evaluation of Commercial Thermography Systems for Quantitative Composite Inspection Applications," The Second Joint NASA/FAA/DoD Conference on Aging Aircraft, August 31, - September 3, 1998, Williamsburg, Virginia, USA.
3. Roach, Dennis P., Rackow, Kirk A., "An Experiment to Assess Flaw Detection in Composite Honeycomb Structures", American Society of Nondestructive Testing Fall Conference Proceedings October 16-20, 2000, Indianapolis, Indiana, USA.
4. Hexcel Corporation, Publication Number, HTU285, "HexTOOL® M81 User Guide", < http://www.hexcel.com/Resources/UserGuides/ > HEXTOOL_ M81_UserGuide.pdf, page 6, March 2009.
5. Hexcel Corporation, Publication "HexWeb® EC Engineered Core", <www.hexcel.com>, page 3. March 2009.
6. Journiac, Sophie, "Simulation of Ultrasonic Inspection of Composite Using Bulk Waves: Application to Curved Components", 6th Group Research 2501and 9th Anglo-French Physical Acoustics Joint Conference IOP Publishing, Journal of Physics: Conference Series 269 (2011).
7. North Star Imaging Incorporated website ,< http://www.xviewct.com/industrial-ct-scans/aerospace-and-aviation/aerospace-honeycomb-structure >, April 2011.
8. Han, Xiaoyan, Favro, L.D. and Thomas,R.L. "Thermal Wave NDI of Disbonds and Corrosion in Aircraft", Wayne State University, Institute for Manufacturing Research and Department of Physics, Detroit, MI 48202, U.S.A.
9. Thermal Wave Imaging Incorporated website, "EchoTherm® Operating Characteristics Publication", < http://www.thermalwave.com/echotherm.htm >, Copyright 2010.